Development 129, 5789-5801

doi:10.1242/dev.00155

Cell lineage analysis of the amphipod crustacean *Parhyale hawaiensis* reveals an early restriction of cell fates

Matthias Gerberding[1,3], William E. Browne[2] and Nipam H. Patel[1,3,*]

[1]Department of Organismal Biology and Anatomy, University of Chicago, Chicago, IL 60637, USA
[2]Department of Molecular Genetics and Cell Biology, University of Chicago, Chicago, IL 60637, USA
[3]Howard Hughes Medical Institute, University of Chicago, Chicago, IL 60637, USA
*Author for correspondence (e-mail: npatel@midway.uchicago.edu)

Accepted 11 September 2002

SUMMARY

In the amphipod crustacean, *Parhyale hawaiensis*, the first few embryonic cleavages are total and generate a stereotypical arrangement of cells. In particular, at the eight-cell stage there are four macromeres and four micromeres, and each of these cells is uniquely identifiable. We describe our studies of the cell fate pattern of these eight blastomeres, and find that the eight clones resulting from these cells set up distinct cell lineages that differ in terms of proliferation, migration and cell fate. Remarkably, the cell fate of each blastomere is restricted to a single germ layer. The ectoderm originates from three of the macromeres, while the remaining macromere generates the visceral mesoderm. Two of the micromeres generate the somatic mesoderm, a third micromere generates the endoderm and the fourth micromere generates the germline. These findings demonstrate for the first time a total cleavage pattern in an arthropod which results in an invariant cell fate of the blastomeres, but notably, the cell lineage pattern of *Parhyale* reported shows no clear resemblance to those found in spiralians, nematodes or deuterostomes. Finally, the techniques we have developed for the analysis of *Parhyale* development suggest that this arthropod may be particularly useful for future functional analyses of crustacean development.

Key words: Pattern formation, Cell lineage, Fate map, Crustacea, *Parhyale*

INTRODUCTION

In the early embryos of several animals, such as nematodes, ascidians and leeches, complete cell cleavages generate individual cells whose fates have been determined either by following cells in living animals or through the injection of various tracers (Sulston, 1981; Nishida, 1987; Weisblat et al., 1984). In these taxa, specific patterns of invariant cell lineage are found, and thus individual cells (blastomeres) of the early embryo contribute to distinct parts of the organism. Subsequent studies, especially in the nematode *C. elegans*, have revealed that these lineage patterns are generated through a wide variety of mechanisms, including the asymmetric distribution of cellular components and cell-cell signaling between groups of cells whose positions are highly reproducible. By contrast, most insects, including *Drosophila*, display superficial cleavage and lack patterns of invariant cell lineages during early cleavage stages. The early development of this insect is generally characterized as one in which positional information plays the major role in cell fate decisions, although invariant cell lineages are found much later in *Drosophila* development, particularly within the nervous system.

Many crustaceans (and a small number of insects), however, do display total cleavage during early embryogenesis, but very few studies have been undertaken to determine the extent to which invariant cell lineages occur in these animals. In some cases, observations based on tracking cell morphologies in crustacean embryos have suggested the presence of invariant lineages (Grobben, 1879; Bigelow, 1902; Fuchs, 1914; Hertzler et al., 1992), and a single study making use of the injection of a tracer has demonstrated the origin of mesendoderm material from a single blastomere at the four-cell stage in the indirect developing shrimp *Sicyonia* (Hertzler et al., 1994).

In this study, we describe experiments designed to trace the cell lineage pattern in the amphipod crustacean, *Parhyale hawaiensis*. Previous authors have noted the unique arrangement of blastomeres found in this group of crustaceans, but had not established lineage data (Langenbeck, 1898; Weygoldt, 1958; Scholtz, 1990). In amphipods, the first and second cell divisions are slightly unequal, but the third division is highly unequal and thus generates a set of four macromeres and four micromeres. Through the injection of various lineage tracers into the blastomeres of the eight-cell stage embryo, we demonstrate that the fates of the macromeres and micromeres in *Parhyale* are restricted to individual germ layers. The ectoderm is generated by three macromeres, the visceral mesoderm by the fourth macromere, the somatic mesoderm is generated by two micromeres, and the endoderm and the germ cells are generated by the two other micromeres. With the

notable exception of germline formation in some insects (Kahle, 1908), this is the first demonstration of distinct blastomere cell fates in an arthropod. There is, however, no obvious resemblance between the lineage patterns of *Parhyale* and those of the nematodes, spiralians and deuterostomes, the lineages of which are known. Thus, it would appear that this level of blastomere fate determination has evolved independently in this group of crustaceans. Finally, we believe that this crustacean has several properties, including ease of culturing, ready accessibility to all embryonic stages and relatively rapid generation time, that make it a useful system for detailed analyses of many aspects of crustacean development.

MATERIALS AND METHODS

Preparation of embryos for injection

Parhyale hawaiensis is a direct-developing marine amphipod that is simple to raise and propagate year-round in the laboratory, and we are currently preparing a detailed description of its care and embryonic staging (W. B., M. G., A. P. and N. P., unpublished). *Parhyale hawaiensis* embryogenesis takes approximately 10.5 days at 26°C and below is a very brief description of the stages that are relevant to this study.

The first three cleavages take place within the first 8 hours of development and result in an eight-cell embryo composed of four macromeres and four micromeres (Fig. 1A,B). By 12 hours, there are roughly 100 cells distributed relatively evenly at the surface of the egg (Fig. 1C) and all the cells are approaching the same size (as the macromeres have divided more than the micromeres). At 18 hours many of the cells have condensed towards specific regions of the egg and the onset of gastrulation begins shortly after this, as some cells move to more internal position within the egg. At ~3 days (Fig. 1D), a distinct germband with head lobes is visible. At this time, the ectodermal cells begin to arrange themselves into a precise pattern of rows and columns, and this organizational process proceeds in an anterior-to-posterior direction across the germband. The initial rows that are formed undergo a subsequent precise pattern of divisions to yield individual parasegments, and again these divisions progress anterior to posterior along the germband. At 4 days (Fig. 1E), the germband has lengthened considerably and is folded in its posterior region, and appendages are clearly visible in the anterior regions of the animal. At 6 days (Fig. 1F), all the appendages are visible and internal organs such as the gut can be seen forming. At 9 days (Fig. 1G) organogenesis appears nearly complete, and the embryo has the same morphology as a hatchling, which in turn is very similar in morphology to a full grown adult (Fig. 1H).

In our study, we injected the blastomeres of two-, four- and eight-cell stage embryos to track their lineage. TF-4 needles (World Precision Instruments) are pulled with a horizontal puller P-90 (Sutter) and filled with the appropriate labeled dextran or mRNA. To keep them in place during the injection, the embryos are placed on a slide next to small strip of 2% agar in 50% seawater. Once properly oriented, the embryos are injected with an IM 300 Microinjector (Narishige) on a Zeiss Axiovert microscope. The following tracers were used: rhodamine-conjugated dextran [2.0 μg/μl TRITC dextran (M_r 500,000), Sigma], fluorescein-conjugated dextran [2.0 μg/μl FITC dextran M_r 150,000) Sigma], Biotin-conjugated dextran [Biotin dextran, 1 μg/μl (70,000 M_r), Sigma], and capped mRNA (1 μg/μl) encoding either green fluorescent protein (GFP) or *Discosoma* Red fluorescent protein (DsRed.T1) (Bevis and Glick, 2001). For double injections of fluorescent tracers, several embryos were injected with one tracer, the location of the tracer was confirmed by fluorescence microscopy, the embryos were placed back on a slide, oriented appropriately and injected for a second time (in a different cell) with a different tracer.

Biotin-coupled dextran as single tracer

The embryos injected with Biotin dextran were fixed in one of two ways, either by formaldehyde fixation or by boiling. Fixation by formaldehyde is done for 15 minutes in 3.7% formaldehyde in PBS (pH 7.0) at room temperature. While in the fixation solution, a hole was poked in the egg and the two outer membranes were removed with tungsten needles. When fixed in this manner (and stained as described below), it was possible to further dissect the embryos and flatten them afterwards on a slide; the tissue and the yolk stayed white and the DAPI staining was bright and clear. However, because a hole must be made initially, on either the ventral or the dorsal side, the distribution of clones could be scored accurately only on side or the other side. Fixation by boiling was achieved by immersing the embryos for 10 seconds in 95°C PBS (pH 7.0) followed by transfer to ice-cold PBS. This method of fixation makes dissections easier, the two membranes can be easily removed without damaging the embryo, and the whole embryo can be scored from all sides. However, the boiling hardens the embryos so that they cannot be flattened later, it turns the yolk a yellow color, and the DAPI staining of boiled embryos is weaker and has more background than that of formaldehyde-fixed embryos. After either method of fixation, embryos were incubated with HRP-conjugated streptavidin (Molecular Probes) at a dilution of 1:1000 in PT (PBS + 0.01% Triton), washed in PBS, developed with 1 mg/ml DAB + 0.6 mg/ml NiCl + 0.01% H_2O_2 for 10 minutes, washed in PBS, stained with DAPI at 1 μg/μl in PBS, and cleared in 50% and 70% glycerol in 1×PBS. Pictures were taken with a Zeiss Axiophot using a Kontron 3012 (Jenoptik) digital camera. Data were assembled using Adobe Photoshop 6.0.

Fluorochrome-coupled dextrans and mRNAs for DsRed and GFP as single and double tracers

The embryos injected with fluorochrome-coupled dextrans or mRNA for the fluorescent proteins EGFP or DsRed.T1 can be scored live over the whole period of embryogenesis. Pictures were taken at approximately 12 hours, 18 hours (just before gastrulation), 3 days (germband) and 6 days (organogenesis). Pictures were taken with a Zeiss Axiophot using a Sony digital camera. Data were assembled using Adobe Photoshop 6.0.

FITC dextran has a higher background problem because of tissue autofluorescence than does TRITC dextran. mRNAs for the fluorescent proteins EGFP and DsRed.T1 were made from expression vectors that were made by cloning the GFP- and DsRed.T1-coding regions from pEGFP-1 (Clontech) and pDsRed.T1 (Bevis and Glick, 2001) into the expression vector pSP (gift of Angus MacNicol) and capped transcripts generated using the SP6 Ambion mMessageMachine kit. Expression was detected by fluorescence 1.5 hours after injection of DsRed.T1 mRNA and 2-3 hours for EGFP mRNA. The GFP signal was relatively weak in our hands, although the DsRed.T1 signal was as strong as the signal from TRITC labeled dextrans.

Relative merits of histochemistry versus fluorescence

Biotin dextran is a useful tracer because, after fixation and subsequent enzymatic development, there is a high signal/noise ratio and the preparations are permanent. The Biotin dextran method also has a spatial resolution at the single cell level and allows for simultaneous DAPI staining. The main drawback of the Biotin dextran method is that embryos must be fixed, and thus each injection yields data for only a single time point. Fluorescent tracers are useful as they allow for continuous in vivo observation of the clones. However, this method does not allow us to collect DAPI data simultaneously, and there is a loss of fluorescent signal upon fixation. TRITC dextran and FITC dextran labeling provide excellent spatial resolution until gastrulation; after that, this technique does not produce as good a spatial resolution

as the Biotin dextran method (although this may be resolved by improved optical techniques). The fluorescent proteins GFP and DsRed.T1 show the same advantages and disadvantages as the fluorochromes. In some cases, we have used a 1:1 mix of Biotin dextran plus one of the fluorescent tracers to take advantage of the strengths of each technique.

RESULTS

Each macromere and micromere of the eight-cell stage can be identified individually, labeled and shown to contribute to only one of the germ layers

During the first 8-9 hours of development, three complete cleavages of the *Parhyale* embryo result in the formation of an eight-cell embryo (Fig. 1A). It is the third cleavage that is highly asymmetric and yields the eight-cell pattern of four macromeres and four micromeres. The individual macromeres and micromeres can be distinguished according to their size, morphology and contacts made with neighboring cells (Fig. 1A). We have named these cells in accordance with their eventual progeny (Fig. 1B, see below). The smallest macromere is named 'Mv', the other three macromeres, when viewed from the dorsal side, are named clockwise 'Er', 'Ep' and 'El' (Fig. 1B). The smallest micromere (which is the sister cell of the smallest macromere 'Mv') is named 'g', and this micromere has the most prominent nucleus of all the micromeres. The other three micromeres, when viewed from the dorsal side, are named clockwise (starting from 'g') 'mr', 'en' and 'ml' (Fig. 1B). As the next few paragraphs will demonstrate, the prospective fate of the blastomeres is distributed in the following way: 'Mv' generates all of the visceral mesoderm. 'El', 'Ep' and 'Er' generate three different portions of the ectoderm (roughly distributed anterior left, posterior and anterior right, respectively, in the later embryo). The cells of the 'g' clone are the germ cells. 'ml' and 'mr' generate the left and right regions of the somatic mesoderm, respectively. 'en' generates the endoderm.

In our initial experiments, we injected individual cells of the eight-cell embryo with either Biotin-dextran or DsRed.T1 mRNA as lineage tracers (see Materials and Methods). We then analyzed the distribution of clones in germband stages (3-4 days of development) and during organogenesis (6-7 days of development). Table 1 summarizes the number of clones analyzed at various stages for each injected blastomere. The fate of 'El', 'Ep', 'Er', 'ml' and 'mr' is easy to recognize at the germband stage, but the fate of 'g', 'en' and 'Mv' only become clear at about 6 days of development when organ formation has begun. Having established the fate of these clones, we then went back to analyze the distribution, proliferation and migration of the clones during earlier stages (between the time of injection and the establishment of the germband at 2-3 days). Below, we begin with a description of the fate of the clones at the germband and organogenesis stages, and then describe the way in which these clones behave and move during earlier stages of development.

The ectoderm is a composite of the macromere clones 'El', 'Er' and 'Ep'

The progeny of 'El', 'Er' and 'Ep' are strictly ectodermal; all

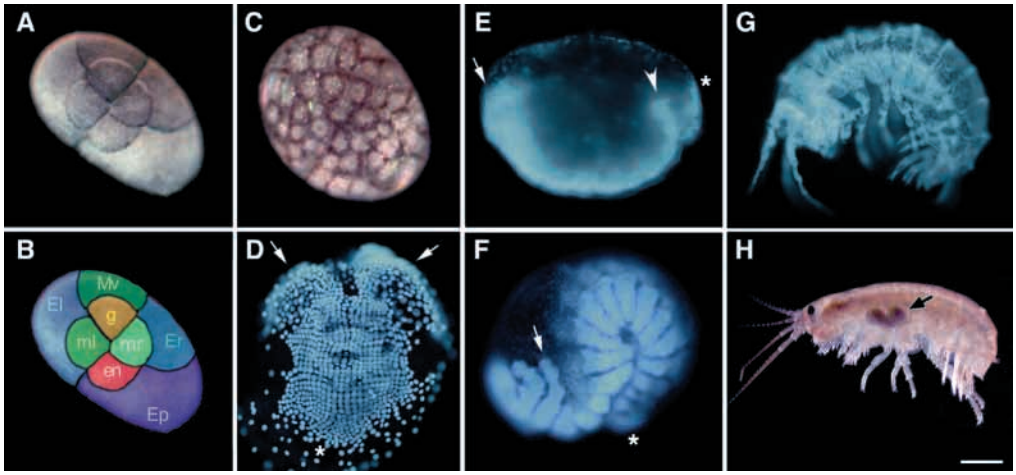

Fig. 1. Overview of *Parhyale* development. (A) Living eight-cell embryo. Dorsal view, anterior upwards. After the third division, there are four macromeres and four micromeres. (B) The nomenclature of the macromeres and micromeres projected on the egg of (A). The smallest macromere is called 'Mv', the other macromeres moving clockwise are called 'Er', 'Ep' and 'El'. The smallest micromere (sister of 'Mv') is called 'g', the other micromeres moving clockwise are called 'mr', 'en' and 'ml'. (C) Dorsal view of a living egg at 12 hours. This stage is nicknamed the 'soccerball' stage, and at this stage there are ~100 superficially located cells of roughly the same size. (D-G) DAPI stained embryos. (D) The early germband at day 3. Ventral view, anterior upwards. The first landmarks of the germ band are the head lobes (arrows). At this stage, the trunk ectoderm is organizing itself into a remarkably precise grid of rows and columns, with each initial row giving rise eventually to a single parasegment of the animal. Cells are still being added to the germband at the posterior (asterisk). The overall organization shows a marked AP gradient of development. (E-H) Lateral views, anterior leftwards. (E) Germband extension at day 4. As the germband extends, it acquires a sharp ventral infolding (arrowhead; head indicated by arrow, telson by asterisk). In this embryo, the segments anterior to the fifth thoracic segment and posterior to approximately the middle of the abdomen are at the ventral surface of the egg, while the remaining thoracic and abdominal segments are within the infolded region. (F) The extended germband at day 5. The infolding has extended to the point where only the telson and segments anterior to the mandible still lie at the ventral surface of the egg. At this stage, the appendages are distinct from the body wall (second antenna marked by arrow, telson by asterisk). (G) The embryo at day 9. By this time, the adult morphology has been established as *Parhyale* is a direct developer (compare with H). (H) A living gravid adult female carrying eggs in her ventral brood pouch (arrow). Scale bar: 100 μm in A-G; 2 mm in H.

Table 1. Blastomere injections

	Blastomeres								
	'Er'	'El'	'Ep'	'Mv'	'mr'	'ml'	'en'	'g'	Total
Single injections									
Biotin-dextran*	4	9	6	7	9	8	5	8	56
TRITC or FITC†	n.a.	n.a.	n.a.	4	3	3	2	1	13
DsRed.T1 mRNA‡	2	2	2	3	3	2	2	3	19
Double injections									
TRITC+FITC dextran§	3	3	4	3	2	2	4	1	22
Total	9	14	12	17	17	15	13	13	**110**

Numbers indicate how many clones were injected as a blastomere with either biotin-dextran, fluorescent-dextran or DsRed.T1 mRNA and analyzed at later stages.

*Cells were injected with biotin-dextran and embryos were fixed and analyzed at the germband stage or later

†Endoderm and visceral mesoderm progenitors were injected with either TRITC- or FITC-labeled dextran and pictures were taken throughout embryogenesis. (No numbers are given for the experiments for TRITC and FITC dextran-injected ectodermal blastomeres, as the resolution with these labels after gastrulation is relatively poor, although what was seen agreed perfectly with the the data obtained using other tracers.)

‡Cells were injected with mRNA for *Discosoma* red fluorescent protein and pictures were taken throughout embryogenesis

§One cell was injected with TRITC-labeled dextran, another one with FITC-labeled dextran. Pictures were taken throughout embryogenesis for endoderm and visceral mesoderm, and up through gastrulation for germline, ectoderm and somatic mesoderm.

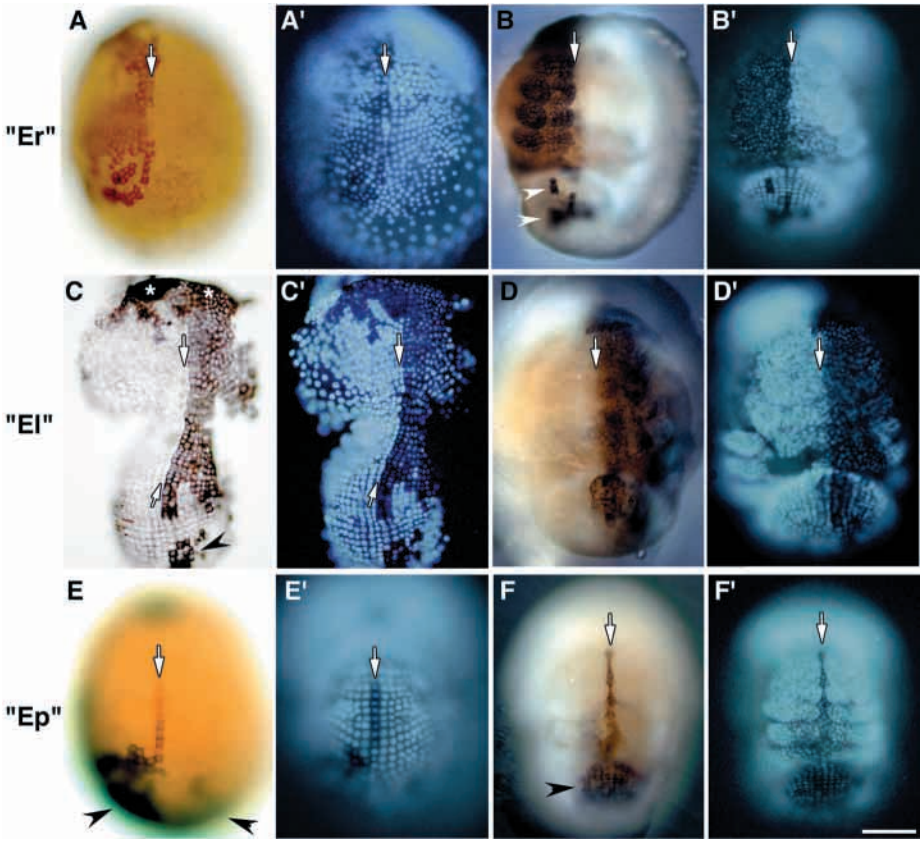

Fig. 2. Development of ectoderm clones during germband formation. Ventral views, anterior upwards. Arrows denote the location of the midline. Top, middle and bottom rows show the three ectoderm clones resulting from injecting macromeres 'Er', 'El' and 'Ep', respectively. Anterior-right and anterior-left clones originate from 'Er' and 'El', respectively, and an unpaired posterior bilateral ectoderm clone originates from 'Ep'. The distribution of these clones is complementary and their allocation to the three regions obeys strict rules in the gnathal and thoracic segments. In more anterior and more posterior segments, these rules are less strictly implemented (see text). (A-F) Brightfield images showing the Biotin-dextran injected clones. (A′-F′) corresponding DAPI images. (A,B) The 'Er' clone. Injection of 'Er' gives an anterior ectoderm clone that is restricted to the right part of the embryo in the gnathal and thoracic segments. (A,A′) Day 3. The ectodermal cells start to organize themselves into a regular grid pattern to which 'Er' contributes the anterior right region. (B,B′) Day 4.5. The anterior ectoderm is composed of ventral neuroectoderm and lateral and dorsal appendage and body wall ectoderm. 'Er' has contributed the right part of all these regions of the anterior ectoderm. This clone has also contributed some scattered cells (arrowheads) to the posterior ectoderm, which still shows a grid-like arrangement. (C-D′) The 'El' clone. Injection of 'El' gives an anterior ectoderm clone that is restricted to the left part of the embryo in the gnathal and thoracic segments. (C,C′) Day 3.5. Dissected germband preparation showing that the 'El' clone is restricted to the left side in the thorax and abdomen, but is on both sides in the anterior part of the head (asterisks on the left and right sides). Scattered contribution can also be seen in the more posterior ectoderm (arrowhead). (D,D′) Day 4.5. 'El' is contributing the left part of the anterior ectoderm in a way that is complementary to 'Er'. (E,F) The 'Ep' clone. Injection of 'Ep' gives an unpaired posterior ectodermal clone that is excluded from the gnathal segments, is restricted to the single column of midline cells in the thoracic segments, and is bilateral throughout the abdomen. (E,E′) Day 3.5. 'Ep' is contributing to the midline of the thorax during the initial assembly of the grid pattern, as well as to the posterior ectoderm of the abdomen (arrowheads). (F,F′) Day 4.5. 'Ep' contributes to the thoracic midline plus the majority of the abdominal ectoderm. Owing to the infolding of the embryo, only the contribution to the most posterior part of the abdomen is visible here (arrowhead). Scale bar: 100 μm.

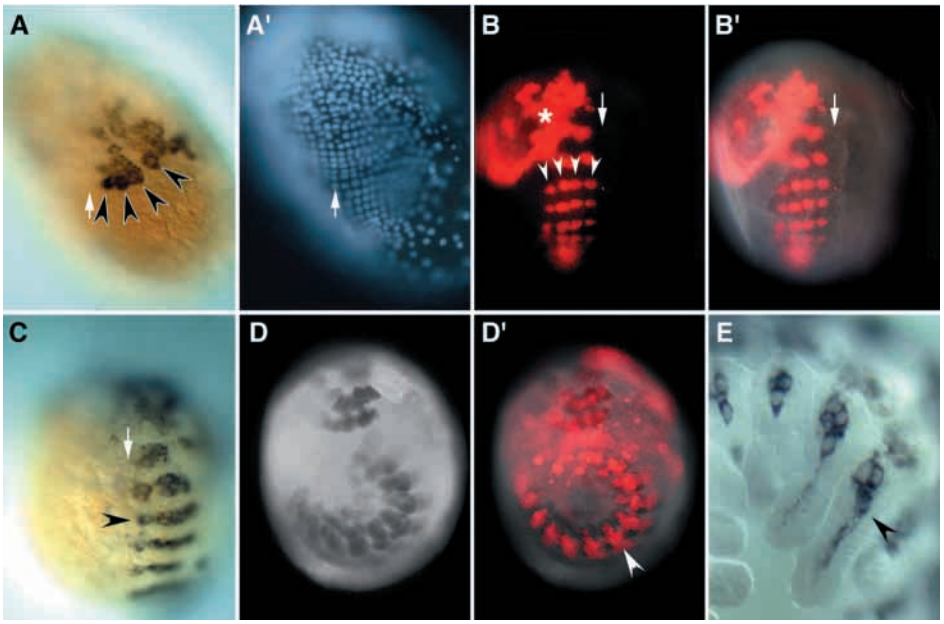

Fig. 3. Development of the somatic mesoderm clones. (A-C) Ventral views, (D) lateral view. Arrows indicate the location of the midline. There are two unilateral mesodermal clones of left somatic and right somatic mesoderm derived from micromeres 'ml' and 'mr', respectively. (A) The mesoderm at day 3. Concomitant with the formation of the grid in the surface layer of the ectoderm, the internal mesoderm clones (here an 'ml' clone) of each side generate an irregular array of cells that will contribute to the head mesoderm, plus four so-called mesoteloblasts (arrowheads). The mesoteloblasts are stem cells that in turn generate the segmental somatic mesoderm of all segments posterior to the mandible. (A′) DAPI image of A, but focused more ventrally to reveal the overlying ectodermal grid. (B,B′) The mesoderm at day 3.5. Living DsRed.T1 labeled 'mr' clone, with the fluorescent image alone shown in B and overlaid with the brightfield image in B′. The four mesoteloblasts have generated several rows of segmental somatic mesoderm, each comprising four cells (arrowheads). The more anterior, non-teloblastic mesoderm occupies lateral, rounded domains within the head (asterisk marks one edge of this domain). (C) The mesoderm at day 4: Biotin-dextran label of an 'ml' clone. The number of mesoderm cells per segment increases as the initial four cells in each segment proliferate (arrowhead). (D,D′) The mesoderm at day 5. Living TRITC dextran labeled 'ml' clone, with the brightfield image alone shown in D and overlaid with the fluorescent image in D′. The segmental mesoderm has started to populate the appendages (arrowhead). (E) Biotin dextran label of 'ml' at day 6. High magnification view shows the mesoderm within several developing appendages.

their progeny are restricted to the ectoderm (and ectodermal derivatives such as the nervous system) and the entire ectoderm can be traced back to these three macromeres.

At ~3 days, when the initial germband is well organized, the cells from 'El' and 'Er' make up, respectively, the anterior left and anterior right ectoderm of the germband, and arrange themselves into a very precise pattern of rows and columns of cells (Fig. 2A,C). The 'Ep' clone forms the posterior ectoderm of the germband (Fig. 2E), the cells of this clone will also eventually organize into rows and columns, but do so later than the more anterior ectoderm (Fig. 2F). In addition, the cells of the 'Ep' clone also produce the midline of the ectoderm extending all the way up to the gnathal region of the embryo, and thus generate the central midline that separates the 'El' and 'Er' clones (Fig. 2E,F) along much of the length of the embryo. Interestingly, distinct behaviors of midline cells have also been found at later stages of development in the amphipod *Orchestia* (Gerberding and Scholtz, 1999; Gerberding and Scholtz, 2001).

The 'El', 'Ep' and 'Er' clones intermix but remain a monolayer. As the germband first begins to form, 'El' and 'Er' form clones with a relatively small cell size and high cell density positioned at the anterior part of the forming germband. By contrast, the 'Ep' clone displays a relatively larger cell size and lower cell density and is spread out over a region of the posterior ventral side and most of the posterior dorsal side of the egg; as the germband continues to condense, the 'Ep' clone proliferates and compacts to form the most posterior part of the germband (data not shown). Given that the germband is formed by the condensation of cells from the surface of the egg, it is not surprising that some mixing of the cells between the three clones does occur, but the mixing is restricted in a predictable way. In the head (anterior to the future gnathal region), there is no distinct midline and cells from 'El' and 'Er' mix extensively across the midline. In the region of the gnathal and thoracic segments, however, the 'Ep' clone establishes a well-defined midline, and the 'El' and 'Er' clones maintain a strictly left-right distinction (Fig. 2A-D). The anteroposterior boundary between 'El'+'Er' domain versus the 'Ep' clone varies from embryo to embryo, but is generally somewhere within the posterior thorax or anterior abdomen, in a few cases the contribution of 'Ep' can be surprisingly small (Fig. 2B,D,F). Possibly, this variability in the composition of the germband ectoderm from the three clones results from the variable degree of inequality in the first and second cleavages that determine the relative sizes of the different macromeres. This boundary is usually quite irregular (i.e. not defined by any specific row of cells), and in addition, there can be scattered cells from 'El' and 'Er' that end up incorporated in a random manner into the developing abdomen. In summary, 'El', 'Er' and 'Ep' clones can be characterized as occupying anterior left, anterior right and posterior ectoderm, respectively, but with some expected patterns of mixing occurring.

The somatic mesoderm is a composite of the micromere clones 'ml' and 'mr'

The 'ml' and 'mr' clones were analyzed during germband formation and organogenesis and were found to generate the somatic mesoderm and produce no other cell type than somatic mesoderm.

The germband mesoderm is assembled out of two clones. At the germband stage, the clones originating from 'ml' and 'mr'

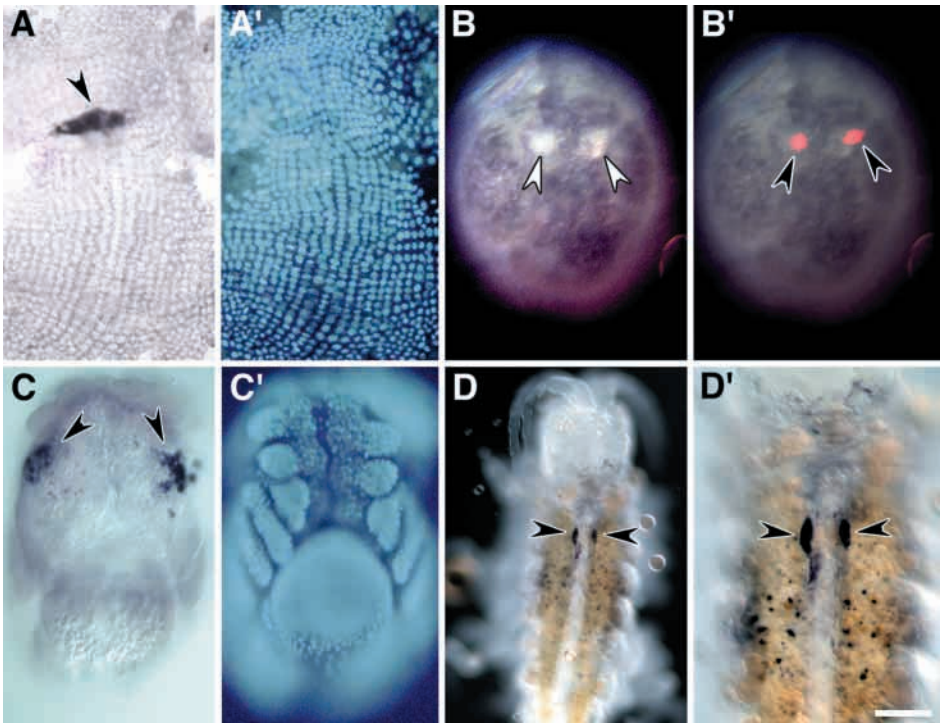

Fig. 4. Germ cell clones. The 'g' micromere generates an unpaired bilateral germ cell clone that splits at mid-embryogenesis and populates the paired gonads. (A,A′) The germ cells at day 3. The early migration of the germ cells from dorsal to ventral stops at germ band formation. The germ cells (arrowhead) form a single medially located internal cluster at the level of the mandibular segment. (A) Brightfield image showing the cluster of the three to five germ cells (arrowhead). (A′) Corresponding DAPI image, but focused more ventrally on the ectodermal grid. (B,B′) The germ cells at day 4. During germ band extension, the cluster splits into two halves that migrate laterally. (B) Brightfield image of a living embryo containing a DsRed.T1 mRNA labeled 'g' clone. Even in brightfield only images of uninjected embryos, the germ cell clusters (white arrowhead) always stand out as they are more reflective than the surrounding cells. (B′) Corresponding brightfield plus fluorescent images overlay. The DsRed.T1-labeled germ cells (arrowhead) are within the bright clusters seen in B. (C,C′) The germ cells at day 4.5. The germ cells are migrating towards the dorsal side from day 4 to day 7. (C) Brightfield image of the Biotin dextran-labeled clone. During this stage of lateral migration, the germ cells (arrowheads) seem to lose adherence to each other and migrate as single cells. (C′) Corresponding DAPI image of C, but focused more ventrally on the head appendages to show that the germ clusters are still within the gnathal region. (D) The germ cells at day 9. The two right and left germ cell clusters now populate the paired gonads (arrowheads). (D′) Higher magnification view. The scattered black spots represent spurious DAB precipitation in the yolk. Scale bar: 80 μm in A-C′,D; 100 μm in B,B′; 40 μm in D′.

are found immediately underneath the ectoderm (Fig. 3A). The cells originating from 'ml' and 'mr' are found on the left and right sides of the embryo respectively, and we never observed any violation of this left-right allocation. At day 3, each unilateral clone is subdivided into two populations, one consists of a randomly arranged anterior population of cells (non-teloblastic mesoderm) that will form the mesoderm of the head and heart, and the second is a stereotypically arranged set of posterior cells (teloblastic mesoderm) that will go on to form all the rest of the somatic mesoderm (Fig. 3A,B).

The anterior, non-teloblastic parts of the 'ml' and 'mr' clones form the mesoderm of head (and its associated appendages) and two distinct circular structures on either side of the head that are not associated with segments or appendages (Fig. 3B). During organogenesis, these circles disperse and the cells migrate dorsally (Fig. 3D), moving jointly with endoderm and visceral mesoderm (see below). Before hatching, labeled cells can also be found mediodorsally in the putative heart rudiment (data not shown).

The posterior region of the mesoderm is the teloblastic mesoderm. On each side of the embryo, four mesodermal stem cells called mesoteloblasts differentiate at the very posterior end of the clones (Fig. 3A). As these stem cell divide, they move posteriorly one segment at a time in the embryo, leaving behind a row of four progeny in each segment as they do so. This establishes a pattern of four mesodermal precursor cells per segment on each side of the embryo (Fig. 3B). By day 4.5, the mesoteloblasts have finished the generation of segmental mesoderm progeny. These segmental mesodermal progeny then begin to divide (Fig. 3C) and eventually form the muscle cells of the appendages and body wall (Fig. 3D,E).

The germ cells originate from micromere 'g'

The lineage of 'g' is restricted to the germ line and there is no other source for the germ cells. During development, the 'g' clone settles at the prospective gonads.

During early germband formation at day 3, the cells in the 'g' clone lie in single cluster underneath the ectoderm at the level of the future mandibular segment (Fig. 4A). As development proceeds, the clone splits at the midline into two bilaterally symmetric populations of cells (Fig. 4B) and by day 4 reach a position lateral to the germband at the level of the future gnathal segments (Fig. 4C). The two clusters of cells derived from 'g' keep migrating until they reach the dorsal median where the heart rudiment forms. By day 9, the cells of the 'g' clone are found within the developing gonads in a dorsal position adjacent to the gut at the level of the fourth thoracic segment (Fig. 4D), and it is at this position that the ovaries and testes are centered in adult animals.

The endoderm originates from micromere 'en' and the visceral mesoderm originates from macromere 'Mv'

The fate of 'en' and 'Mv' clones is most obvious during

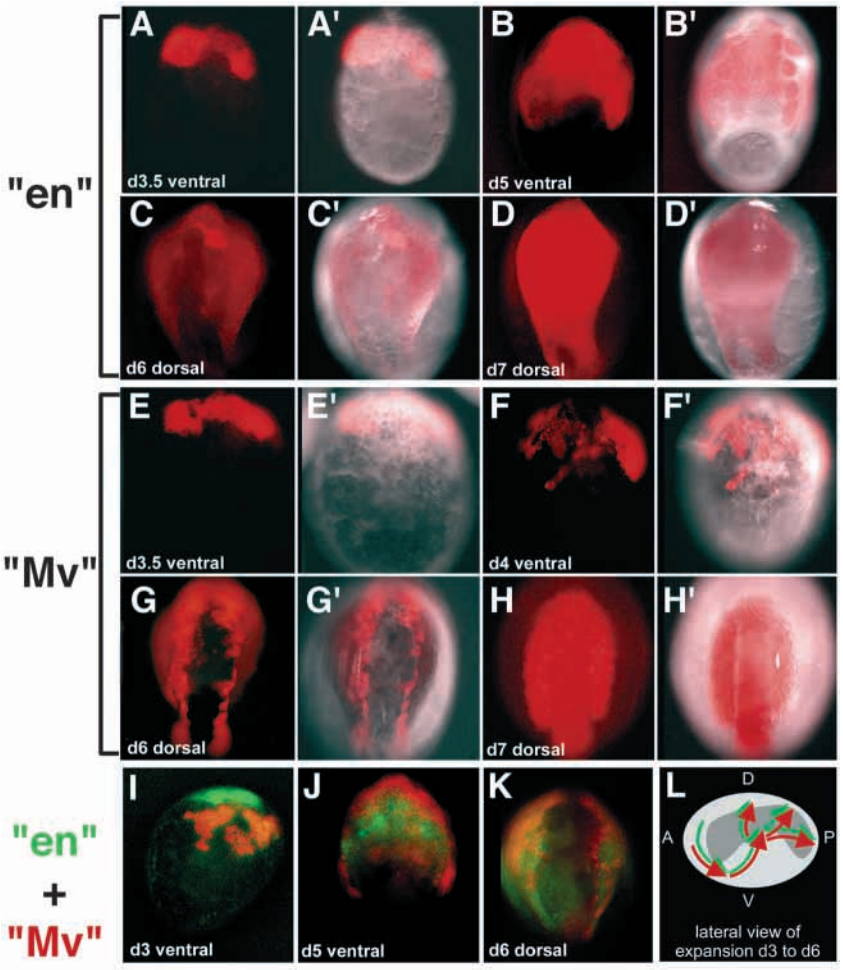

Fig. 5. The development of the endoderm and the visceral mesoderm. The gut is composed of two clones, an unpaired bilateral clone for the midgut endoderm that is derived from micromere 'en', and an unpaired bilateral clone for the visceral mesoderm derived from macromere 'Mv'. (A-H) Fluorescent images of TRITC dextran clones. (A′-H′) Same fluorescent images, but overlaid with the corresponding brightfield images. (A-D) TRITC dextran labels of the endoderm progenitor 'en'. (A) The 'en' clone at day 3.5, ventral view: the clone is situated dorsally and anterior and starts to from an internal layer that expands posteriorly. (B) The 'en' clone at day 5, ventral view: the clone has expanded underneath the germband ectoderm and mesoderm forming a continuous ventral layer. (C) The 'en' clone at day 6, dorsal view: cells of the clone spread dorsally to envelope the yolk and form the tube structure of the midgut. (D) The 'en' clone at day 7, dorsal view: the clone has enclosed the yolk completely. (E-H) Single labels of the visceral mesoderm progenitor 'Mv'. (E) The 'Mv' clone at day 3.5, ventral view: the clone is on the egg surface and lies anterior of the ectoderm material. (F) The 'Mv' clone at day 4, ventral view: the clone is forming an internal layer and is migrating laterally and posteriorly. (G) The 'Mv' clone at day 6, dorsal view: the clone is enclosing the yolk and endoderm (see below), and individual cells have processes that extend dorsally. (H) The clone at day 7, dorsal view: the clone has completely enclosed the yolk at the same time as the 'en' clone. (I-K) Double labels of both 'en' (red, TRITC dextran) and 'Mv' (green, FITC dextran). (I) The clones at day 3, ventral view: during germband formation, the clones occupy different areas; 'en' is dorsal and anterior to 'Mv'. (J) The clones at day 5, ventral view: both clones have moved extensively, with the 'Mv' cells now located ventral and external to the 'en' cells (K) The clones at day 6, dorsal view: during the closure of the gut tube, the endoderm of 'en' is internal to the visceral mesoderm 'Mv'. (L) Schematic view on of the expansion of 'en' (red arrows) and 'Mv' (green arrows) between day 3 and day 6. Lateral view, anterior leftwards, dorsal upwards, yolk in gray. At days 3-6, both clones move to the ventral side and then form a joint sheath that moves laterally and back to the dorsal side enclosing the yolk.

organogenesis (6-7 days). At this stage, it is clear that 'en' and 'Mv' generate the gut, i.e. endoderm and visceral mesoderm. Endoderm and visceral mesoderm are in immediate proximity and therefore so close together that overlap can not be exclude in all cases. However, the variety of methods used all provide evidence that 'en' generates the entire endoderm and 'Mv' generates the entire visceral mesoderm, and the lineages are restricted to these tissues respectively.

During organogenesis, the endoderm and visceral mesoderm clones form the gut tube around a central yolk. The central yolk is formed early by a separation of the outer cytoplasm from the inner yolk. The redistribution of the cytoplasm can easily be visualized as all the three dextran-coupled tracers as well as the DsRed protein are found preferentially in the cytoplasm. From the one-cell to the eight-cell stage, cytoplasmic signal is found throughout the whole injected cell. Starting at the 16-cell stage, the cytoplasm becomes successively localized at the surface and excluded from the inner yolk. This observation, however, does not allow us to conclude whether the inner yolk is cellular or acellular. If the yolk is cellular, the yolk cells could either originate from cells that stay central from early on or from cells that settle within the yolk secondarily. Alternatively, an acellular yolk could be formed by having the cells divide without a corresponding nuclear division. Indeed, previous observations of dissociated cells from early embryos of gammarid amphipods suggested that the cytoplasm and the yolk become separated by tangential divisions of the cells without divisions of their nuclei, resulting in small outer cells with cytoplasm and nuclei, and a bigger inner yolk compartment that is anuclear (Rappaport, 1960).

At germband formation, the 'en' clone comprises no more than eight cells (data not shown). The clone is the most dorsal clone and its cells are flat and spread out over the dorsal yolk. At the same time, the 'Mv' clone comprises about two dozens of cells and is located between the ectoderm clones of 'Er' and 'El' and the dorsal 'en' clone (data not shown). During formation of the midgut, the 'en' clone extends ventrally and posteriorly from its initial dorsal anterior position (Fig. 5A-D), while the 'Mv' clone extends dorsally and posteriorly from its initial anterior lateral position (Fig. 5E-G). During this

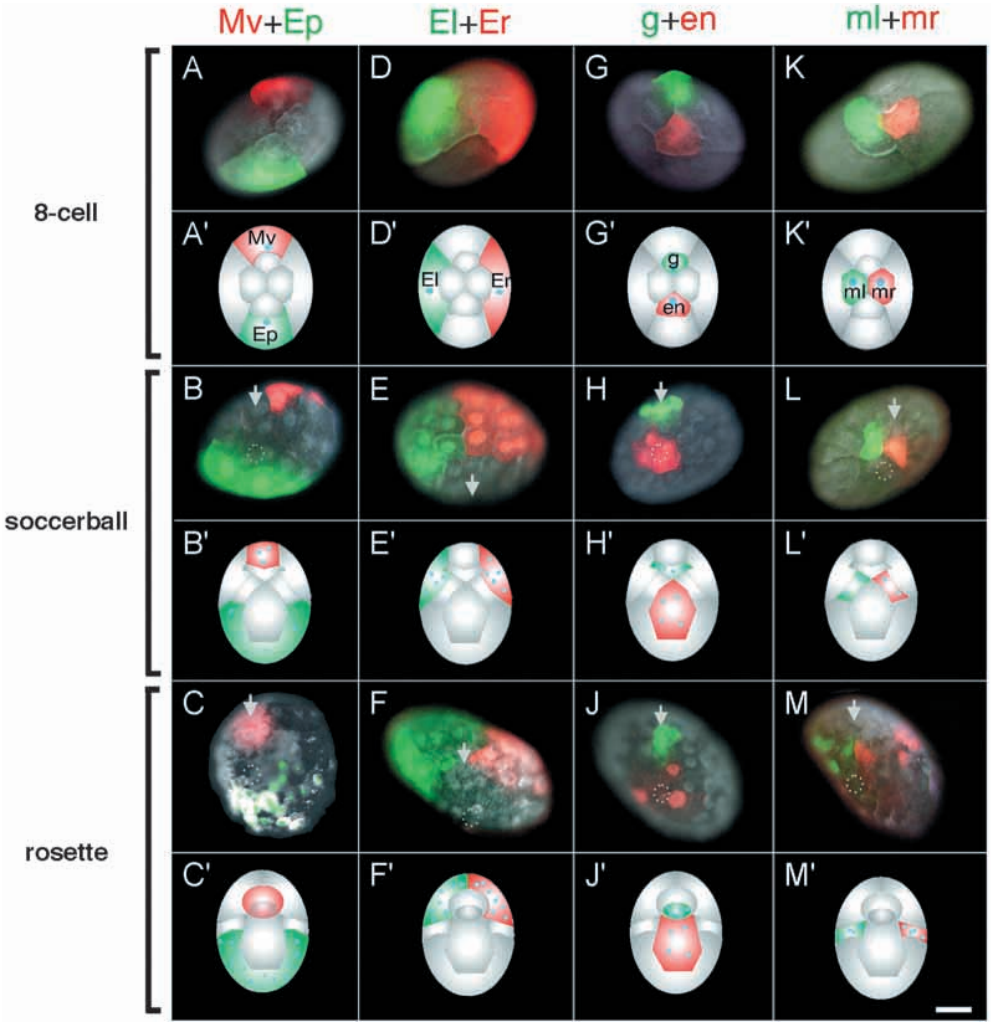

Fig. 6. Proliferation and migration of clones up to gastrulation. Pairs of opposing macromeres and micromeres were injected at the eight-cell stage and relative positions were scored at the soccerball stage and at gastrulation. (A-M) Embryos that have been double injected with TRITC dextran and FITC dextran. Pictures are triple exposures for brightfield and the two fluorescent channels for the injected dyes. Because the eggs have variable shapes and are photographed at slightly different orientations to maximize the visibility of the clones, the position of the anterior edge of the germ cells and center of the endoderm cell region are marked by an arrow and broken circle, respectively, in order to facilitate the comparison of the panels. Among the early eggs, the angle between the longitudinal axis and the AP axis is variable, but most frequently, the angle is ~45°. Note that there are two different arrangements of cells that show mirror symmetry as seen in G versus K. (A′-M′) Schematic drawings. The drawings integrate the distribution of clones found in (A-M) and in other experiments. The data are projected onto an idealized embryo with a single aligned longitudinal egg axis and embryonic AP axis. Blue dots indicate approximate numbers of nuclei. (A-C) The 'Mv'+'Ep' pair. (B) 'Mv' proliferates slower than 'Ep'. (C) 'Mv' forms the deeper (internal) part of the rosette, while 'Ep' covers the superficial dorsal posterior region of the egg. (D-F) The 'El'+'Er' pair. (E) 'El' and 'Er' proliferate at the same rate. Note that this embryo is rotated so far that the endoderm cells are out of the field of view. (F) 'El' and 'Er' are situated to both sides (left and right) and ventral to the rosette. (G-J) The 'g'+'en' pair. (G) The 'g' clone forms a cluster of small cells that divides very little all the way up to hatching. (J) The 'g' clone migrates and forms the superficial (outer) part of the rosette. The 'en' cells become flat and spread out. (K-M) The 'ml'+'mr' pair. (L) 'ml' and 'mr' cells divide very little until after gastrulation. (M) 'ml' and 'mr' cells are lined up adjacent to the ectoderm clones. Scale bar: 100 μm in A-H; 80 μm in I-K.

movement, both clones extend together and the leading edge comprises cell of both clones. In double labels with FITC- and TRITC-labeled dextrans, however, it is clear that 'en' cells are situated internal to the 'Mv' cells (Fig. 5J-L). At the end of this extension process, 'en' and 'Mv' form the two layered sheath of midgut around a tube-shaped yolk mass (Fig. 5D,H). We also analyzed sections through the midgut of labeled 7-day-old embryos to confirm that the 'en'-derived cells were internal to the 'Mv'-derived cells (data not shown).

The clones show distinct proliferation and migration patterns prior to germband formation

Having analyzed the cell fate of each of the four macromere and four micromere lineages at germband and later stages, we decided to investigate some earlier stages in order to understand more about the behavior of these lineages in the steps leading up to the formation of the initial germband. We focused our analyses on two stages. First, at 12 hours of development, at which time the cells are more or less uniformly distributed around the surface of the egg (Fig. 1C, Fig. 6B). Owing to the appearance of the embryo at this time, we have nicknamed this the 'soccerball' stage. Second, at 18 hours of development, when gastrulation is just about to begin. At this stage, there is a rosette shaped cluster of cells that is easily visible in living embryos (Fig. 6C), and we have nicknamed this the 'rosette' stage.

The events prior to germband formation are addressed by double fluorescent labels. Because there are no clear morphological landmarks for orienting the embryo at the soccerball stage, it is difficult to compare the position of individually labeled clones. In addition, the overall shape of the egg at this stage does not provide a reproducible way of orienting the embryo forming within. However, by injecting pairs of blastomeres with different tracers (one with

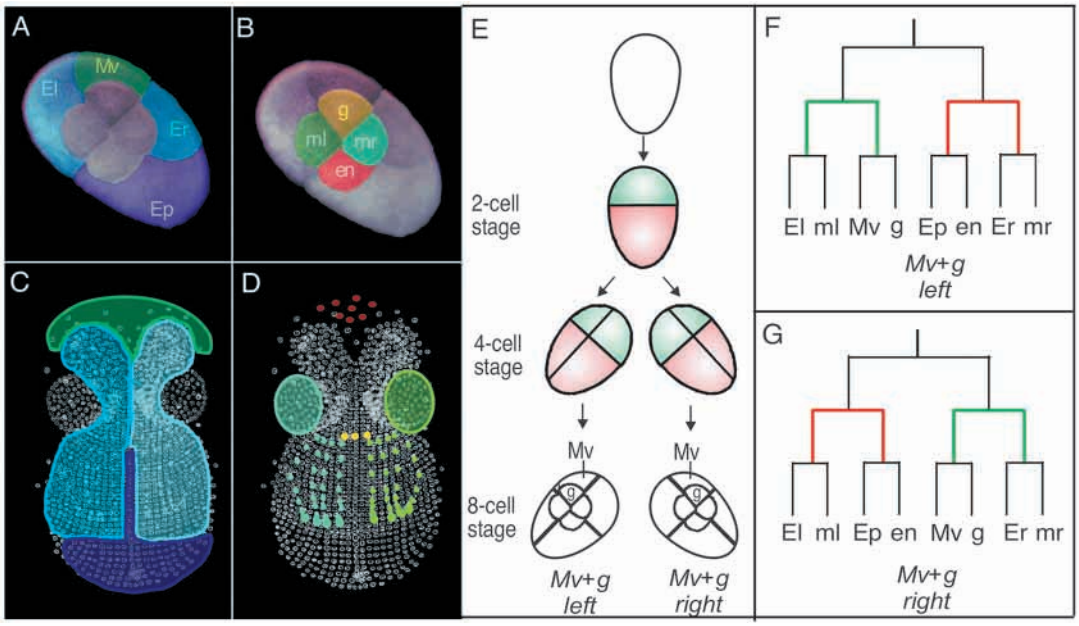

Fig. 7. Fate map and mirror symmetry of the blastomeres. (A,B) Dorsal view at the eight-cell stage with the macromeres highlighted in A and the micromeres highlighted in B. (C,D) Schematic of an early germband stage embryo (ventral view), with the fates of the macromere progeny illustrated in C and the micromere fates illustrated in D. (C) 'Mv' (green) produces the visceral mesoderm, 'Er', 'Ep' and 'El' (dark blue, purple and light blue, respectively) produce the anterior right, posterior and anterior left ectoderm respectively. The progeny of these four macromeres are still located on the surface at the early germband stage; the 'Mv' clone is internalized later. (D) 'g' (yellow) produces the germ cells, 'mr', 'en' and 'ml' (dark green, red and light green, respectively) contribute the right somatic mesoderm, the endoderm and the left somatic mesoderm, respectively. The cells of the four clones are already internalized (lying underneath the superficial layer of cells) by germband formation. [Germband in C,D is adapted from Weygoldt (Weygoldt, 1958).] Note that we show the eight-cell stage from the dorsal side as the micromeres would otherwise not be visible from a ventral view, and show the germband embryo from the ventral side, as this is the standard orientation for illustrating arthropod embryos. (E) First, second and third cleavage. The first cleavage (which gives rise to the two-cell stage) is transversal and slightly unequal, the second cleavage (which gives rise to the four-cell stage) is longitudinal and slightly unequal as well. Variation in the location of the furrow of the second cleavage is the cause of two different arrangements at the four-cell and eight-cell stages that show mirror symmetry. At the four-cell stage, sister pairs are indicated by common colors (red shading versus green shading). The third cleavage (which gives rise to the eight-cell stage) is latitudinal and highly unequal, and gives rise to the distinction between macromeres and micromeres. (F,G) Cell pedigrees of the two arrangements at the eight-cell stage. The sister cells 'Mv' and 'g' either share a progenitor with 'Er' and 'mr' or with 'El' and 'ml'. Note that in either arrangement, the relative location of germ layer progenitors is still the same.

FITC dextran and another with TRITC dextran, see also row four of Table 1) we found that we could understand the relative orientation of all the clones. The 'Mv'+'Ep' and 'g'+'en' pairs are situated along the AP axis, and the AP axis is the line connecting them. The 'El'+'Er' and 'ml'+'mr' pairs are situated to the right and the left side of the AP axis, therefore the line connecting them is perpendicular to the AP axis.

Proliferation rates and relative area are different between clones and change over time within clones. During the 4 hours between the eight-cell stage and the 100-cell soccerball stage, the numbers of cells, in each clone, the area on the egg surface that they cover, and their relative locations are all changing simultaneously. At the soccerball stage, 'El', 'Ep' and 'Er' comprise about 12 to 15 cells (Fig. 6E), 'Mv' comprises about eight cells (Fig. 6B). The micromeres have undergone two to three divisions, and thus there are four to eight progeny of each micromere at the soccerball stage (Fig. 6H,L). At the eight-cell stage, the macromeres of course cover a greater area than the micromeres. By the soccerball stage, progeny of the three macromeres 'El', 'Ep' and 'Er' have increased their area relative to the progeny of macromere 'Mv'. The progeny of micromere 'en' increase their area of coverage relative to the other micromere lineages (Fig. 6H).

Migration patterns are different between clones. Relative to each other, the clones move extensively up to the formation of the germband and beyond. The clone that is proliferating and moving the least seems to be the 'en' clone; thus, we define the position of the 'en' clone to be fixed, and describe the movements of the other cells relative to the 'en' clone. After the eight-cell stage, the progeny of the three other micromeres, 'mr', 'g' and 'ml', leave their dorsal and superficial positions next to 'en' and migrate to ventral and internal positions. During the movements, they pass through the anterior tip of the egg. The 'g' clone takes a medial path and crosses over the 'Mv' clone (Fig. 6H,J). The 'mr' and 'ml' cells take lateral paths (right and left) and do not cross the progeny of 'Mv' (Fig. 6L,M). The two macromeres 'Er' and 'El' expand from their ventromedial position towards the anterior tip of the egg (Fig. 6E,F). The 'Ep' cells follow 'Er' and 'El' anteriorly, but remain posterior to them at all times (Fig. 6B,C). In terms of movements, the behavior of the 'Mv' clone is similar to the 'en' clone in that its cells move very little and remain superficial until germband formation (Fig. 6B,C).

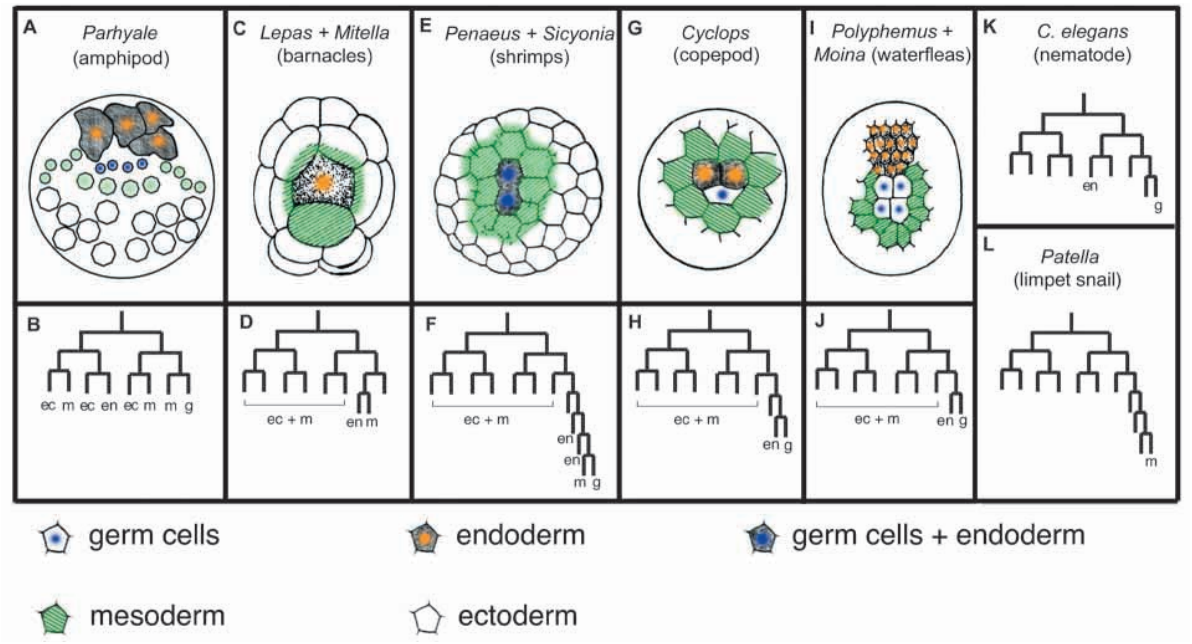

Fig. 8. Crustacean fate maps and various cell lineages. (A,C,E,G,I) Fate maps from crustacean taxa that possess total cleavage. The fate maps show the arrangements of the mesoderm, endoderm and germ cells at the time of the gastrulation. The fate map of *Parhyale* is derived from the lineage tracing data described here. All other fate maps were conceived from staining whole embryos and looking at the differential morphology and location of cells. By definition, the position of initial cell ingression is defined as the blastopore. The blastopore, however, is at different places in different crustaceans. The blastopore is anterior in *Parhyale*, posterior in barnacles, shrimps and copepods, and ventral in waterfleas. Therefore, the panels show ventral views, anterior upwards in A,I, and posterior views, dorsal upwards in C,E,G. Although *Parhyale* is a malacostracan crustacean like shrimps, its fate map (A) is less similar to that of shrimps (E) and more similar to those of non-malacostracans (C,G,I). In all four taxa, the endoderm progenitors (gray cells with blue nuclei) or joint endoderm+germline progenitors (gray cells with yellow nuclei) are situated in front of the mesoderm progenitors (green cells). Moreover, in *Parhyale* (A), *Cyclops* (G) and the waterfleas (I), the endoderm and mesoderm encircle the germ cells (white cells with blue nuclei). The fate map of the malacostracan shrimps (E) places the endoderm dorsal of the mesoderm. Most other malacostracans have superficial cleavage and the mesoderm is positioned anterior of the endoderm (not shown). (B,D,F,H,J) Crustacean cell lineages. Again, other than for the work reported here for *Parhyale*, cell fate in the crustacean cell lineages has been inferred from cell morphologies and is not based on tracing experiments. The number of divisions before the putative progenitors for mesoderm, endoderm and germ cells (m, en, g) are specified varies across the taxa from three in the amphipod, four in barnacles and five in the copepod, to seven in shrimps. The germline emerges as a sister of either the endoderm or the mesoderm but not the ectoderm (ec), but has not been recognized in early barnacle embryos. (K,L) Nematode and spiralian cell lineages. In *C. elegans*, the endoderm is specified after the third division. In *Patella*, the primary mesoderm is specified after the sixth division. Data are based on the following: (A,B) malacostracan amphipod *Parhyale* (this study); (C,D) maxillopodan barnacles (Bigelow, 1902; Shiino, 1957); (E,F) malacostracan shrimps (Kajishima, 1951; Hertzler, 2002); (G,H) maxillipodan copepod (Fuchs, 1914) (the relationship between the AP axis and the endoderm and germline that is shown here is modeled after other crustaceans); (I,J) branchiopodan waterfleas (Grobben, 1879; Kühn, 1913); (K) nematode *C. elegans* (Sulston et al., 1983); and (L) limpet snail *Patella* (Dictus and Damen, 1997).

During the rosette stage, the somatic mesoderm ingresses laterally, the endoderm remains superficial. At the rosette stage, the cleavage mode changes to superficial cleavage and cells start to condense at two locations. One of these condensations has the shape of a rosette that consists of about 15 cells and is situated at the future dorsal side. The rosette can be further subdivided into a central, deeper ring of cells and an outer, more superficial ring of cells. The other condensation appears a bit later than the rosette and is located at the future ventral side of the embryo. It comprises more cells than does the rosette, but all these cells remain superficial. Double labels elucidate the differential contributions of the clones to these two condensations. The deeper cells of the rosette are the ‘Mv’ progeny (Fig. 6C,J). Double labels of ‘El’+‘Er’ show that the ventral condensation initially comprises cells derived from ‘El’ and ‘Er’. The cells joining it later and more posterior originate from ‘Ep’ (data not shown). Double labels of ‘ml’ and ‘mr’ show that the progenitors for the somatic mesoderm ingress separately at the anterior-right and anterior-left edge of the ventral condensation a few hours after the rosette stage (data not shown). The ‘en’ clone remains superficial throughout the soccerball stage and only ingresses during the germband stage.

The first, second and third cleavage set up the macromeres and micromeres as well as the AP and DV axes

Through the observation of living embryos and the injection of tracers into two- and four-cell embryos, we were also able to deduce the division pattern that leads to the eight-cell stage (data not shown). A summary of the results is shown in Fig. 7.

There are two arrangements of the blastomeres at the eight-cell stage that show mirror symmetry (Fig. 7E). In one case, the sister cells ‘Mv’ and ‘g’ are located to the left of the prospective AP axis, in the other case, they are located to the right. The two arrangements also affect the cell pedigree. If ‘Mv’ and ‘g’ are to the left, they share a common progenitor

at the two-cell stage with ‘Er’ and ‘mr’ (Fig. 7F). If they are located to the right, they share a progenitor with ‘El’ and ‘ml’ (Fig. 7G). Note that this does not affect the architecture of the pedigree, in both cases, each of the two cells at the two-cell stage generates paired ectoderm and mesoderm progenitors and non-paired progenitors for either ectoderm and endoderm or mesoderm and germ cells. A similar mirror symmetry pattern during early cleavage that still yields identical embryos has also been reported for other crustaceans and for spiralians (Baldass, 1941; Luetjens, 1995).

Some progenitors for the germ layers are paired, some unpaired. The four clones derived from macromeres ‘Mv’ and ‘Ep’ and micromeres ‘g’ and ‘en’ demarcate the AP axis of the embryo and start as bilateral cell populations situated on the median axis. Conversely, the four clones derived from macromeres ‘El’ and ‘Er’ and micromeres ‘ml’ and ‘mr’ begin as unilateral cell populations on either the left or the right side of the embryo. The ‘ml’ and ‘mr’ clones maintain their perfect left/right allocation while the ‘El’ and ‘Er’ clones display some left/right mixing (see above).

The blastomeres at the eight-cell stage can be depicted as a fate map that predicts where the daughters of the blastomeres end up at the germband (Fig. 7A-D). At the eight-cell stage, the material for the germ layers is located along the AP axis in the following orientation: ‘Mv’ most anterior; ‘g’; ‘Er’/‘mr’/‘ml’/‘El’ in the middle; ‘en’; ‘Ep’ most posterior (Fig. 7A,C). At the germband stage (i.e. after the initial processes of proliferation, migration and mesoderm ingression), the material is reconfigured along the AP axis. The order then is endoderm ‘en’, visceral mesoderm ‘Mv’, anterior ectoderm ‘El’+‘Er’, germ cells ‘g’ and somatic mesoderm ‘ml’+‘mr’ (underneath ‘El’ + ‘Er’), and ‘Ep’ derived ectoderm at the posterior (Fig. 7B,D). During organogenesis, there are further rearrangments so that the endoderm ‘en’ and visceral mesoderm ‘Mv’ have formed the midgut, which runs almost the entire length of the embryo.

DISCUSSION

We labeled specific blastomeres at the eight-cell stage in the crustacean *Parhyale hawaiensis* and analyzed the resulting clones at subsequent stages. In each of the eight-cell lineages, patterns of proliferation, changes in shape and migration are distinct and invariant. More surprising, each blastomere contributes to only one of the germ layers. Each of the eight cells after the third cleavage gives rise exclusively to either germline, ectoderm, mesoderm or endoderm. The germ layers are derived from either one cell, as in the case of the germ cells and the endoderm, or three cells, as in the case of the mesoderm and the ectoderm. In short, the main features of the cell lineage patterns in *Parhyale* are their simplicity and their exclusivity. This is the first time that arthropod blastomere cell lineages have been followed through germband formation up to hatching. Our results provide new material for the study of the evolution of arthropod development. The findings can also be used to analyze the independent evolution of cell lineages in the Bilateria and the extent to which they share common features. Finally, we believe that our results indicate that *Parhyale* may be a useful system for the study of many aspects of crustacean development and suggest that experimental manipulations may be possible in this organism that are not feasible in arthropods with superficial cleavage.

How do the comprehensive data on *Parhyale* compare to the partial fate maps and cell lineages of other crustaceans?

Previous studies of crustacean development had established early fate maps for several species (reviewed by Shiino, 1957; Anderson, 1973; Weygoldt, 1994). With one exception, these fate maps are not the result of labeled lineage analysis, but instead are based on tracing cells of particular morphology during the first few division of the embryo (and usually in sectioned material). For example, in several species, germline cell are picked out because of the unique appearance of the cytoplasm and their relatively slow proliferation rate and the endoderm is picked out by its very internal position in the embryo. Furthermore, these lineage analyses do not follow the fate of the cells up to the time that the final body plan is established. While these fates maps are incomplete, and need to be tested by the injection of lineage tracers, they nevertheless help to illustrate the diversity seen in early crustacean development (Weygoldt, 1979). The fate map and cell lineage pattern we have established here for *Parhyale* bears similarities to that in other crustaceans, but surprisingly not to those of closely related malacostracan taxa, but instead to those of more distantly related non-malacostracan taxa.

Crustaceans are generally divided into five major groups of largely unresolved evolutionary relation, Remipedia, Cephalocarida, Branchiopoda, Maxillopoda and Malacostraca, and it is the latter to which *Parhyale* belongs. Our results allow us to establish a fate map for *Parhyale* and compare it with descriptions of other crustacean fate maps at a similar stage. By definition, the position where the prospective mesoderm is internalized is the blastopore. In *Parhyale* the prospective mesoderm ingresses underneath the ectoderm in an arc and thus the blastopore is more like a lip (A. Price and N. Patel, unpublished), while in at least a few other crustaceans a simpler pore-shaped blastopore exists. In *Parhyale*, the prospective endoderm is situated anteriorly of the prospective mesoderm (Fig. 8A). The inner germ layers move beneath the ectoderm from an anterior blastopore. In the closest relatives of the amphipods, the peracaridan malacostracans, the blastopore is located posterior to the ectoderm and the endoderm is located posterior of the mesoderm (McMurrich, 1895; Manton, 1928). In more distantly related malacostracans that have total cleavage, the endoderm is located dorsal, not anterior, to the mesoderm (Fig. 8E) (Taube, 1909; Hertzler, 2002). However, in the case of the branchiopods, the situation is similar to *Parhyale*. The blastopore is posterior, but the endoderm material is situated in front of the mesoderm (Grobben, 1879; Kühn, 1913; Baldass, 1941; Weygoldt, 1994) (Fig. 8C,I). In the maxillopodans (cirripeds and copepods), the situation is like that in *Parhyale* and the branchiopods (Fig. 8C,G) (Bigelow, 1902; Fuchs, 1914; Delsman, 1917; Shiino, 1957). The lack of similarity between the fate map of *Parhyale* and those of more closely related malacostracan crustaceans and its similarity to those of distantly related non-malacostracan crustaceans suggests that this may be an example of convergent evolution.

Heterochrony of germ layer determination

Some cell lineage data, again based usually on tracing cells by their morphology, is also available for several crustacean taxa with total cleavage. In some of the taxa with total cleavage, cleavage is equal in the sense that early blastomeres cannot be distinguished (Müller-Calé, 1913; Benesch, 1969). In others, cleavage is more or less unequal and early blastomeres are distinguishable and are described as progenitors for germ layers. In general, the putative progenitors for mesoderm, endoderm and germ cells are derived from few cells at an early stage. A comparison between *Parhyale* and these other crustaceans reveals that different numbers of cell cycles can occur before lineages are restricted to specific germ layers and different numbers of cells are used to generate the germ layers. For reasons of space, only comparisons for the endoderm and germ line are discussed here.

In the malacostracan shrimp, *Sicyonia*, the endoderm originates jointly with the mesoderm and the germline from one of the four blastomeres after the third division, as the only previous lineage tracer injection experiments carried out in crustaceans shows (Hertzler et al., 1994). The fifth and sixth division at the 31- and 62-cell stage each generate an endoderm progenitor (Fig. 8F) (Hertzler, 2002). In the maxillopodan barnacles, the fourth division at the 16-cell stage generates single progenitors of endoderm and mesoderm, and the endoderm progenitor is considerably bigger than all other cells (Fig. 8C) (Bigelow, 1902; Delsman, 1917; Shiino, 1957; Anderson, 1969) In the branchiopodan waterfleas, the fourth division at the 16-cell stage sets up single endoderm and germline progenitors of average size (Fig. 8I) (Grobben, 1878; Kühn, 1913). In the maxillopodan copepod *Cyclops*, the same process happens at the fifth division at the 32-cell stage (Fig. 8G) (Fuchs, 1914). This five taxa comparison shows that the endoderm progenitor ‘en’ of *Parhyale* is generated earlier than in other crustaceans. In addition, it is a micromere that is the sister of the ectoderm progenitor ‘Ep’ (Fig. 8B); in other crustaceans, however, the endoderm progenitors are either average sized or macromeres and, in lineage terms, are most related to the progenitors of either the mesoderm or the germ line (Fig. 8D,F,H,J).

Similarly, a comparison between our results for *Parhyale* and those for other crustaceans shows that the germ line progenitor ‘g’ in *Parhyale* is generated earlier than in other crustaceans. In *Sicyonia*, the germ cell lineage separates from the mesoderm at the seventh division at the 122-cell stage (Fig. 8F) (Hertzler, 2002). In the barnacles, no germline is detected at the 64-cell stage (Bigelow, 1902; Delsman, 1917; Shiino, 1957; Anderson, 1969). In the waterfleas and copepods, the germline is set up as the sister cell of the endoderm progenitor at the 16- and 32-cell stages, respectively (Fig. 8H,J) (Grobben, 1878; Kühn, 1913; Fuchs, 1914).

These comparisons of the relative timing of cell lineage restrictions can be extended outside the crustaceans as well because the determination of germ layers is an ancient process that dates back to the common ancestor of protostomes and deuterostomes. The insect *Miastor*, a midge, offers an example where a germline progenitor is separated from the rest of the egg at the syncytial eight-cell stage by the deployment of a membrane surrounding only the germline progenitor (Kahle, 1908). Outside of the arthropods, early embryonic patterns of invariant cell lineage are found in species off nematodes, annelids and ascidians. *C. elegans* generates a gut progenitor at the third division and a germline progenitor at the fourth division (Fig. 8K) (Sulston et al., 1981). In basal spiralians, the progenitors for the endoderm and mesoderm are generated at the sixth cell division, in leeches and other clitellates they are generated much later (Fig. 8L); the germline in clitellates is found to descend jointly with the muscle mesoderm from mesoderm stem cells (Goto et al., 1999; Kang et al., 2002). In ascidians, the various germ layers are composed from the combination of many cell lineages of the 64-cell stage; a germline has not been detected by this stage (Nishida, 1987). In conclusion, germ layer determination usually takes place between the third and sixth division and the generation of germ cells can occur much later than this. It is debatable whether there are features of germ layer determination that are homologous between arthropods, nematodes, spiralians and ascidians, but it is clear that the lineage patterns found in *Parhyale* are particularly noteworthy because they occur much earlier than in other animals.

Is the link between the cell lineage and the germ layers in *Parhyale* incidental or functional?

Cell lineage and cell fate are linked to various degrees in different developmental systems (Goldstein and Freeman, 1996; Moody, 1999). The nematode *C. elegans* has an invariant cell lineage, and some aspects of cell fate are linked to cellular asymmetries set up during the pattern of cell division, but other experiments show that several cell fate decisions can be uncoupled from the cell division pattern (Schnabel, 1997). Within annelids, comparisons of cell division patterns that at first appear rather different do reveal the conservation of certain patterns, hinting that a certain series of divisions may be necessary to determine the different cell fates and are therefore conserved during evolution (Schneider et al., 1991; Dohle, 1999). In the frog *Xenopus*, the arrangement of blastomeres varies, but if embryos are selected for a stereotypic arrangement of blastomeres, the resulting lineages are invariant in the sense that blastomere fate is predictable and restricted (Moody, 1987a; Moody, 1987b). However, the fact that there are also non-stereotypical arrangements that give rise to identical animals demonstrates a primacy of regional determinants over cell lineage (Moody, 1990). Although we find a stereotyped arrangement of micromeres and macromeres in *Parhyale*, and an invariant lineage pattern with regards to the formation of different germ layers, we do not know how yet how tightly cell fate is tied to cell lineage in *Parhyale*. The isolation of blastomeres as done in shrimp (Kajishima, 1951; Hertzler et al., 1994; Wang and Clark, 1996), and cell ablation experiments will allow us to investigate this issue and assess the contributions of cell lineage and positional information during *Parhyale* development. In addition to these questions of cell fate determination during early embryogenesis, we believe that *Parhyale* holds promise as a useful crustacean for the investigation of many developmental problems, particularly comparative questions aimed at understanding the evolution of pattern formation within the arthropods.

We thank Carsten Wolff, Gerhard Scholtz and Phil Hertzler for sharing results on *Orchestia* and *Sicyonia* development prior to publication, Mark Martindale and Eric Wieschaus for their suggestions on the use of Biotin dextran and heat fixation respectively,

Angus MacNicol for the pSP plasmid, Brooke Bevis and Ben Glick for the DsRed.T1 plasmid, and Yu-Chiung Wang for his help in constructing the EGFP plasmid for mRNA synthesis. We are especially grateful to Oliver Coleman for identifying the species we work with as *Parhyale hawaiensis*. We also thank Alivia Price for many helpful discussions and contributions including comments on the manuscript, and all the members of the Patel laboratory involved in maintaining our *Parhyale* colony. We thank the anonymous reviewers for their suggestions. M. G. and N. H. P. are, respectively, a research associate and an investigator of Howard Hughes Medical Institute.

REFERENCES

Anderson, D. T. (1969). On the embryology of the cirrepede crustaceans *Tetraclita rosea* (Krauss), *Tetraclita purpurascens* (Wood), *Chthamalus antennatus* (Darwin) and *Chamaesipho columna* (Spengler) and some considerations of crustacean phylogenetic relationships. *Philos. Trans. R. Soc. London B* **256**, 183-235.

Anderson, D. T. (1973). *Embryology and Phylogeny in Annelids and Arthropods*. Oxford: Pergamon Press.

Baldass, F. V. (1941). Die Entwicklung von *Daphnia pulex*. *Zool. Jb. Anat.* **67**, 1-60.

Benesch, R. (1969). Zur Ontogenie und Morphologie von *Artemia salina* L. *Zool. Jb. Anat.* **86**, 307-458.

Bevis, B. J. and Glick, B. S. (2001). Rapidly maturing variants of the *Discosoma* red fluorescent protein (DsRed). *Nat. Biotechnol.* **20**, 83-87.

Bigelow, M. A. (1902). The early development of *Lepas*. *Bull. Mus. Comp. Zool.* **40**, 61-144.

Delsman, H. C. (1917). Die Embryonalentwicklung von *Balanus balanoides* Linn. *Tijd. Nederl. Dierk. Ver.* **15**, 419-520.

Dictus, W. J. and Damen, P. (1997). Cell-lineage and clonal-contribution map of the trochophore larva of *Patella vulgata* (Mollusca). *Mech. Dev.* **61**, 213-226.

Dohle, W. (1999). The ancestral cleavage pattern of the clitellates and its phylogenetic deviations. *Hydrobiologia* **402**, 267-283.

Fuchs, F. (1914). Die Keimblätterentwicklung von *Cyclops viridis* Jurine. *Zool. Jb. Abt.* **38**, 103-156.

Gerberding, M. and Scholtz, G. (1999). Cell lineage of the midline cells in the amphipod crustacean *Orchestia cavimana* (Crustacea, Malacostraca) during formation and separation of the germ band. *Dev. Genes Evol.* **209**, 91-102.

Gerberding, M. and Scholtz, G. (2001). Neurons and glia in the midline of the higher crustacean *Orchestia cavimana* are generated via an invariant cell lineage that comprises a median neuroblast and glial progenitors. *Dev. Biol.* **235**, 397-409.

Goldstein, B. and Freeman, G. (1996). Axis specification in animal development. *BioEssays* **19**, 105-116.

Goto, A., Kitamura, K. and Shimizu, T. (1999). Cell lineage analysis of pattern formation in the Tubifex embryo. I. Segmentation in the mesoderm. *Int. J. Dev. Biol.* **43**, 317-327.

Grobben, C. (1879). Die Entwicklungsgeschichte der *Moina rectirostris*. *Arb. zool. Inst. Wien* **2**, 203-268.

Hertzler, P. L. and Clark, W. H. J. (1992). Cleavage and gastrulation in the shrimp *Sicyonia ingentis*: invagination is accompanied by oriented cell division. *Development* **116**, 127-140.

Hertzler, P. L., Wang, S. W. and Clark, W. H. J. (1994). Mesendoderm cell and archenteron formation in isolated blastomeres from the shrimp *Sicyonia ingentis*. *Dev. Biol.* **164**, 333-344.

Hertzler, P. L. (2002). Development of the mesendoderm in the dendrobranchiate shrimp *Sicyonia ingentis*. *Arthropod Struct. Dev.* **31**, 33-49.

Kahle, W. (1908). Die Paedogenesis der Cecidomyden. *Zoologica* **21**, 1-80.

Kang, D., Pilon, M. and Weisblat, D. A. (2002). Maternal and zygotic expression of a nanos-class gene in the leech *Helobdella robusta*: primordial germ cells arise from segmental mesoderm. *Dev. Biol.* **245**, 28-41.

Kühn, A. (1913). Die Sonderung der Keimesbezirke in der Entwicklung der Sommereier von *Polyphemus*. *Zool. Jb. Anat.* **35**, 243-340.

Langenbeck, C. (1898). Formation of germ layers in the amphipod *Microdeutopus gryllotalpa* Costa. *J. Morphol.* **14**, 301-336.

Luetjens, C. M. and Dorresteijn, A. W. (1995). Multiple, alternative cleavage patterns precede uniform larval morphology during normal development of *Dreissena polymorpha* (Mollusca, Lamellibranchia). *Roux Arch. Dev. Biol.* **205**, 138-149.

Manton, S. M. (1928). On the embryology of a mysid crustacean *Hemimysis lamornae*. *Phil. Trans. R. Soc. London B* **216**, 363-463.

McMurrich, J. P. (1895). Embryology of the isopod Crustacea. *J. Morphol.* **11**, 63-154.

Moody, S. (1987a). Fates of the blastomeres of the 16-cell stage *Xenopus* embryo. *Dev. Biol.* **119**, 560-578.

Moody, S. A. (1987b). Fates of the blastomeres of the 32-cell stage *Xenopus* embryo. *Dev. Biol.* **122**, 300-319.

Moody, S. (1990). Segregation of fate during cleavage of frog (*Xenopus laevis*) blastomeres. *Anat. Embryol.* **182**, 347-362.

Moody, S. (1999). *Cell Lineage and Fate Determination*. San Diego: Academic Press.

Müller-Calé, C. (1913). Über die Entwicklung von *Cypris incongruens*. *Zool. Jb. Anat.* **36**, 113-170.

Nishida, H. (1987). Cell lineage analysis in ascidian embryos by intracellular injection of a tracer enzyme. III. Up to the tissue restricted stage. *Dev. Biol.* **121**, 526-541.

Rappaport, R. J. (1960). The origin and formation of blastoderm cells of gammarid Crustacea. *J. Exp. Zool.* **144**, 43-59.

Schnabel, R. (1997). Why does a nematode have an invariant cell lineage? *Semin. Cell Dev. Biol.* **8**, 341-349.

Schneider, S., Fischer, A. and Dorresteijn, A. W. (1991). A morphometric comparison of dissimilar early development in sibling species of *Platynereis* Annelida Polychaeta. *Roux Arch. Dev. Biol.* **201**, 243-256.

Scholtz, G. (1990). The formation, differentiation and segmentation of the post-naupliar germ band of the amphipod *Gammarus pulex* L. Crustacea Malacostraca Peracarida. *Proc. R. Soc. London B* **239**, 163-211.

Shiino, S. M. (1957). Crustacea. In *Invertebrate Embryology* (ed. M. Kume and K. Dan). pp. 333-338. Tokyo: Bai Fu Kan Press. [English Translation (1988) New York: Garland.]

Sulston, J. E., Schierenberg, E., White, J. G. and Thomson, J. N. (1981). The embryonic cell lineage of the nematode *Caenorhabditis elegans*. *Dev. Biol.* **100**, 64-119.

Taube, E. (1909). Beiträge zur Entwicklungsgeschichte der Euphausiden. I. Die Furchung der Eier bis zur Gastrulation. *Z. Wiss. Zool.* **92**, 427-464.

Wang, S. W. and Clark, W. H. J. (1996). Cell-cell association directed mitotic spindle orientation in the early development of the marine shrimp *Sicyonia ingentis*. *Development* **124**, 773-780.

Weisblat, D. A., Kim, S. Y. and Stent, G. S. (1984). Embryonic origins of cells in the leech *Helobdella triserialis*. *Dev. Biol.* **104**, 65-85.

Weygoldt, P. (1958). Die Embryonalentwicklung des Amphipoden *Gammarus pulex pulex* (L.). *Zool. Jb. Anat.* **77**, 51-110.

Weygoldt, P. (1979). Significance of later embryonic stages and head development in arthropod phylogeny. In *Arthropod Phylogeny* (ed. A. P. Gupta), pp. 107-135. New York: Van Nostrand Reinhold.

Weygoldt, P. (1994). Le développement embryonnaire. In *Traité de Zoologie, Crustacés*, Vol. Tome VII, Fascicule I (ed. J. Forest), pp. 807-899. Paris: Masson.